Platelets Rich Plasma and Imatinib for Ameliorating Liver Fibrosis

Mohamed Mahmoud[a], Walaa G. Hozayen[b], Islam S. Ali[c], Amr E. Ahmed[a], Mohamed M. Elshemy[d], Ayman Hassan[e], Ahmed Nabil[a*]

[a]Biotechnology and Life Sciences Department, Faculty of Postgraduate Studies for Advanced Sciences (PSAS), Beni-Suef University, Beni-Suef, 62514, Egypt.

[b]Biochemistry Department, Faculty of Science, Beni-Suef University, Beni-Suef,62514, Egypt.

[c]Basic Science Department, Delta University for Science and Technology, Gamasa, Dakahlia, Egypt.

[d]Faculty of Science, Menoufia University, Menoufia, Egypt.

[e]Egyptian Liver Research Institute and Hospital , Mansoura, Egypt.

***Corresponding author*:** Ahmed Nabil, Biotechnology and Life Sciences Department, Faculty of Postgraduate Studies for Advanced Sciences (PSAS), Beni-Suef University, Salah Salem St., 62511, Beni Suef, Egypt.**Tel: +201000618349, Email: drnabil_100@psas.bsu.edu.eg**

Abstract:

Background: Hepatic fibrosis is an extreme buildup of extracellular matrix (ECM) proteins like collagen in liver tissues. Imatinib was proven to have promising antifibrotic activity in experimental models through the suppression of platelet-derived growth factor and transforming growth factor. Tyrosine kinases have a principal role in hepatic stellate cells (HSCs) stimulation which finally enhances liver fibrosis. Imatinib as one of the Tyrosine kinases inhibitors family exhibits a great inhibition capacity in controlling HSC activation. On the other hand, Platelet-rich plasma (PRP) represents an autologous product that contains growth factors, immune system messengers, enzymes, and additional factors that have an important role in tissue regeneration. In this report, we studied the anti-fibrotic efficacy of PRP and Imatinib alone or in combination on ameliorating liver fibrosis in an animal model. **Methods:** In this study, Hepatic fibrosis was promoted in rats by the carbon tetrachloride (CCl_4) chemical induction method, then rats were subjected to PRP and Imatinib alone or in combination and finally, liver fibrosis was

evaluated using Masson's Trichrome stain to evaluate collagen fibers quantity in liver tissues. Moreover, hepatic hydroxyproline content was used as a marker for collagen deposition in liver samples. The liver homogenate was also, used for the assessment of different hepatic oxidative stress parameters and MCP-1 inflammatory markers. Cell viability was evaluated using PI stain and the expression of IL6, HGF, and ASMA was detected by RT-PCR. **Results:** Our results showed that the combined therapy of PRP with imatinib was more effective and safer antifibrotic candidate compared to monotherapy as revealed by a significant reduction ($p < 0.001$) in liver hydroxyproline content,fibrosis score, apoptosis, inflammation markers, ASMA, and IL6 gene expression, tissue oxidative stress parameters as well as by the significant increase in HGF gene expression and antioxidant enzymes activity, with minimal changes in liver functions moreover the histopathological examination using Masson's trichrome stain further support our results. **Conclusion:** we suggest that PRP in combination with Imatinib might be a safe and more potent anti-fibrotic combination for liver fibrosis that may allow its use in clinical trials.

Keywords: Liver, Fibrosis, Platelet-rich plasma, Imatinib, Antifibrotic.

Graphical Abstract:

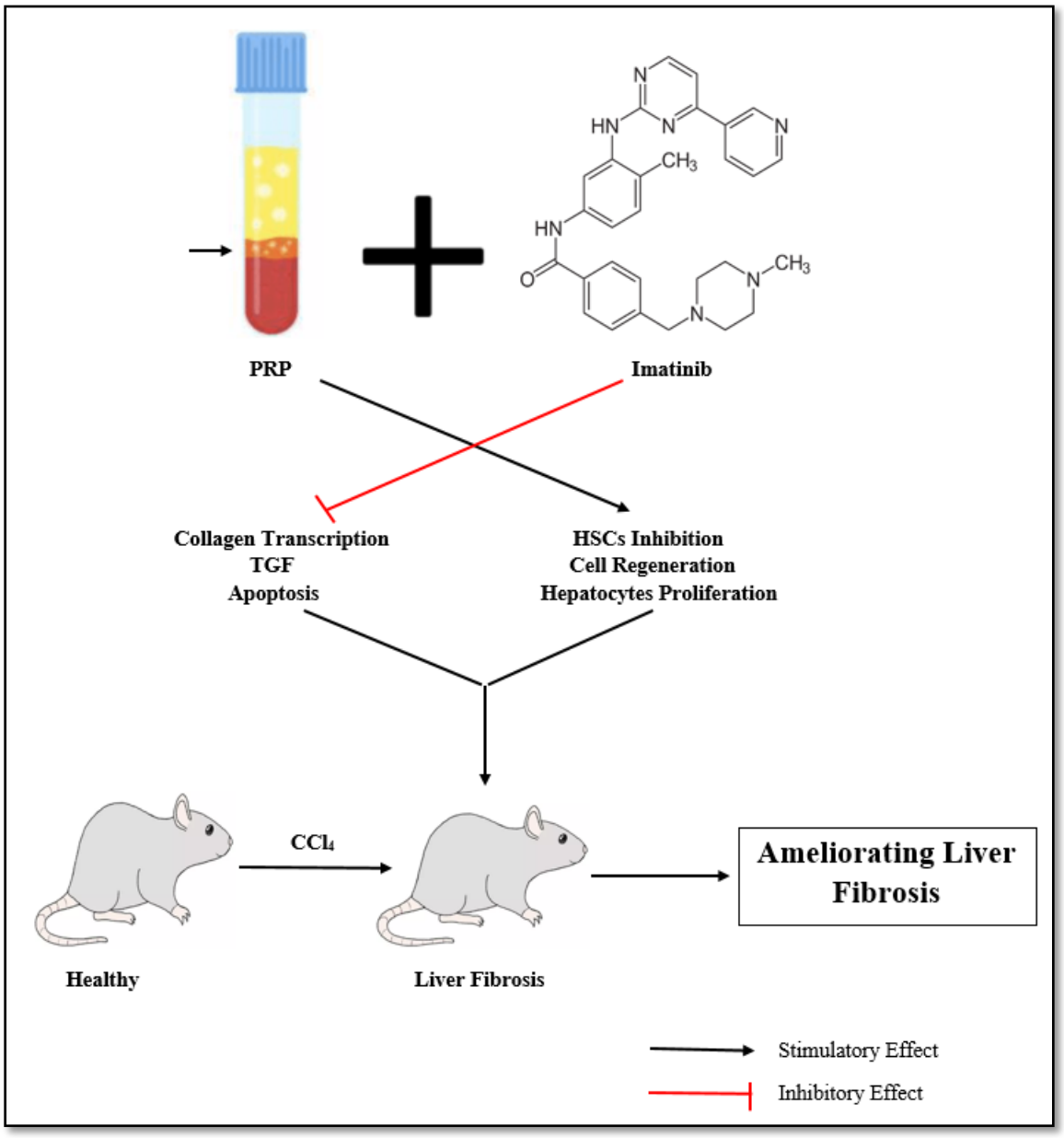

Introduction:

Liver fibrosis is originated from the activation and proliferation of myofibroblasts that activate the Extracellular Matrix (ECM) in the damaged liver. In liver fibrosis, fibroblasts and fibrocytes leads to formation myofibroblasts [1]. Liver transplantation is the most appropriate therapeutic choice for patients suffering from liver failure. However, it is strictly limited by graft rejection, high expense, the shortages of the organ, and needs long-term immunosuppression [2]. Thus, we need a new therapeutic approach to control liver fibrosis.

PRP is defined as a fraction of plasma that contains platelet concentration more than its concentration in the whole blood (1.5 - 8 folds higher than normal platelet count in the blood)[3]. Platelets contain many types of proteins, cytokines, and growth factors, ADP, and ATP. Moreover, PRP contributed to the morpho-functional improvement of damaged organs, maintaining inflammation, enhancing the regeneration mechanisms, and stimulating revascularization [4]. Also, PRP limits fibrosis in many damaged tissues and organs like liver fibrosis by preventing the transition of fibroblast to myofibroblast through downregulation of VEGF-A/VEGFR-1-mediators of TGF-β1/Smad3 signaling pathway [5]. So, PRP seems to have a strong potential for improving the healing and regeneration of body tissues [6], hence PRP is widely used in many areas of regenerative medicine and serves as a promising era for researchers and clinicians.

Tyrosine kinases **(**TKs**)** play regulatory functions in many cellular physiological pathways and they are considered promising targets in the liver fibrosis drug discovery field [7]. TKs have a principal role in hepatic stellate cells (HSCs) stimulation. So, TKs targeting by its inhibitors Tyrosine kinase inhibitors (TKIs) seems to be the best approach to limit HSC activation and manage liver fibrosis [8]. TKIs are therapeutic candidates divided into 3 different generations, which suppress a various types of tyrosine kinases that bind to the tyrosine kinase binding site and decrease its phosphorylation leading to inhibition of stellate cells proliferation [9,10].

Imatinib as one of the TKIs family exhibits a great inhibition capacity in controlling HSC activation. Imatinib mesylate (STI-571) inhibits Bcr-Abl in chronic myeloid leukemia (CML) patients. Many clinical studies demonstrated Imatinib safety in CML treatment and c-Kit-positive gastrointestinal tumors [11]. Moreover, Imatinib inhibits cyclins and cyclin-dependent kinases (CDKs) and stops AKt and ERK phosphorylation, which ameliorates liver fibrosis [12]. So, the purpose of this study is to show the antifibrotic effect of PRP and Imatinib alone or in combination on liver fibrotic rats.

Materials and Methods:

Animals:

Fifty male Sprague–Dawley rats, were used in this study. Their weight was from 170 to 220 gm. Rats were purchased from Medical Experimental Research Center (MERC), Faculty of Medicine, Mansoura University, Egypt. Animals were kept at 8-10 weeks of age at 21°C, 50% relative humidity. Also, housed for 1 week to adapt to the new environment and supplied with water ad-libitum and food. All the animal care procedures and treatments firmly compatible with the Guide for the laboratory Animals usage and care which were published by the US National Institute of Health (Publication No.85–23, revised 1996).

Study design:

These rats were divided into the following groups using SPSS program (Standard version 21). Rats were

divided into 5 groups (10 rats in each group) in a random manner as follows: Group I (Control group): Rats were intraperitoneal injected with corn oil (1 ml/kg) for 9 weeks (2 times per week). Group II (CCl_4 group): Rats were intraperitoneal injected with a solution of 50% (v/v) CCl_4 in Olive Oil (1 ml/kg) for 9 weeks (2 times per week). Group III (CCl_4+ Imatinib mesylate (STI-571)): Rats were intraperitoneal injected with 50% (v/v) CCl_4 in Olive Oil (1 ml/kg) + Imatinib (supplied by Novartis Pharma, Basel, Switzerland) 10 mg/kg per day I.P. at the fifth week of fibrosis induction. Group IV (CCl_4+ PRP): Rats were intraperitoneal injected with 50% (v/v) CCl_4 in Olive Oil (1 ml/kg) + PRP (0.5 mL/kg, twice per week S.C. at the fifth week of fibrosis induction. Group V (CCl_4+ combination): Rats were intraperitoneal injected with 50% (v/v) CCl_4 in Olive Oil (1 ml/kg) + Imatinib 10 mg/kg per day I.P. & PRP (0.5 mL/kg, twice per week S.C.at the fifth week of fibrosis induction.

The rats from the 5 groups were sacrificed with using thiopental anesthetictic agent followed by a laparotomy and hepatectomy. Blood samples were collected by puncturing the heart followed by centrifugation for 15 min (2000 g) for blood serum isolation. The liver tissues were split into 2 halves. One half was preserved in liquid nitrogen and the other half was preserved in HCHO.

Assessment of liver functions:

Serum alanine aminotransferase (ALT) and Albumin (ALB) levels were determined by using kits obtained from Biomed Diagnostics, Cairo, Egypt.

Histopathological analysis:

From each experimental group, histopathological examinations were achieved. After 9 weeks of CCl_4 administration, liver tissues were collected for estimating the score of liver fibrosis. These liver tissues were fixed and cut into sections (10 μm thick), and stained with H & E staining. After that, slides were stained with Masson trichrome for scoring the percentage of collagen and other ECM proteins. Images were prepared from all sections in a random manner, then the percentages of the fibrosis were assessed using the ImageJ software (version 1.6.0_20) [13].

Measurement of Hydroxyproline content:

Liver tissues were minced in hydrochloric acid at 100°C for 24 hours. The hydrolysate cooled, neutralized with NaOH, and centrifuged for 10 mins. The supernatant was added to chloramine T soln and incubated at Room Temperature (RT) (25°C) for 10 mins, then Ehrlich's solution was added. After that, it was incubated at RT for 10 mins, and the optical density (O.D) was assessed at wavelength 560 nm [14].

Estimation of Malondialdehyde (MDA):

1-methyl-2-phenyl-indole was added in acetonitrile which was diluted with CH_3CHO containing $FeCl_3$ to the liver homogenate. After adding 37% (v/v) HCl, samples were mixed and locked with a tight stopper. Then, it was cooled on ice and centrifugation for 10 mins, and the optical density was estimated by using a spectrophotometer at 586 nm [15].

Estimation of Nitric oxide (NO):

The liver homogenate was added to NaOH (0.3 N). For deproteinization, 5% of zinc sulfate was added after incubation for 5 mins at RT. This mixture was got centrifugation for 20 mins, and the then the supernatant was added to 8 mg/ml of VCl3 with Griess reagent and HCl. Samples were estimated at 540 nm spectrophotometrically, after incubation. The nitric oxide

content in samples was determined from $NaNO_3$ standard curve[16].

Estimation of superoxide dismutase (SOD) activity:

The liver homogenate was added with Tris-HCl and pyrogallol. The optical density alteration per 1 minute was measured by checking the raise in the optical density at wavelength (420 nm). We calculated the percentage of inhibition for the samples with the help of a blank tube in the same conditions [17].

Estimation of catalase (CAT) activity:

The liver homogenate was incubated with methanol and H_2O_2 in KH_2P0_4-NaOH buffer in Polystyrene test tubes. The enzymatic reaction started with the addition of a sample containing catalase enzyme. Standard samples consisted of formaldehyde solutions in KH_2P0_4-NaOH buffer. The reaction mixture was incubated for 20 mins at 20°C. The enzymatic reaction ended with the addition of KOH solution to each tube. Then, the tubes were supplied with Purpald in HCl (480 mM) to each tube, and incubated for 10 mins at 20°C. The reaction product was oxidized between Purpald and formaldehyde by addition of potassium periodate in KOH to each tube for obtaining a colored compound. The absorbance was estimated by using a spectrophotometer at 550 nm[18].

Estimation of nitric oxide synthase (NOS) activity:

The liver homogenate was added to L-arginine, NADPH, and hydroxyethyl piperazine ethane sulfonic acid (HEPES) and incubated under constant air bubbling (1 ml/min) for 120 minutes at 37°C. The blank sample contained all the components of the reaction except NADPH. NOS activity was estimated from the difference between blank and samples [19].

Estimation of reduced glutathione (GSH) content:

The liver homogenate and GSSG (or K•PO4 for sample Blank) were added in a cuvette. Place the cuvette in the spectrophotometer. The reaction mixture should be at a specific temperature for the estimation. Add NADPH and mix then read the absorbance at 340 nm. Using the curve linear portion, estimate the rate of decrease and estimate the net rate of the sample by subtracting it from the Blank, where K•PO4 was used instead of GSSG[20].

Estimation of Monocyte Chemoattractant Protein 1 (MCP-1) content:

MCP-1 levels were estimated by using ELISA according to themanufacturer's instruction. The ELISA plates were measured at 450 nm by subtracting background at 570 nm. The MCP-1 concentration was determined from a standard curve and normalized using the values of the respective cell monolayers total protein [21].

Propidium iodide (PI) staining assay:

Portions of liver biopsies were decellularized and the cells (1 to 2×10^6 cells ml^{-1}) were suspended in PBS and got centrifugation at 200g for 5 minutes at RT and the PBS was filtered. The cell pellet was resuspended gently in fluorochrome solution. The tubes were placed at 4°C in the dark for at least 1 hour and at most 24 hours. Cells distribution was analyzed by flow cytometry analysis. For excitation, a 488 nm laser line was used. Red fluorescence (4600 nm) was measured and Gate-out the residual debris. Diploid and hypodiploid DNA peaks were measured [22].

Gene expression of IL6, HGF and ASMA:

A real-time quantitative PCR array was used for the screening. The system of PCR reaction was: 102 μL cDNA synthesis reaction, 1.248 μL RNase, and 1.350 μL 2 × RT2 SYBR Green Master Mix. The conditions of PCR reaction were: 95°C for 10 minutes; 95°C for 15 seconds and 60°C and 1 minute for 40 cycles. After completing the reaction, the melting curve was examined,

at 95°C for 15 seconds, 60°C-95°C for 1 minute [23]. cDNAs were synthesized and followed by RT- PCR reactions. The sequences of PCR primers were shown in (Table 1).

Results:

Effects of Imatinib, PRP mono-therapies, and in combination on liver function tests:

A severe liver injury was caused by CCl_4 administration for 9 weeks which was characterized by a significant hyperactivity of ALT and a significant reduction in ALB concentration. A significant decrease in ALT activity and increase of ALB concentration was observed in the groups treated with PRP, Imatinib, and combined therapy in comparison with group II (CCl_4 group). The treatment with combined therapy showed the most significant reduction in ALT activity and increase in ALB concentration than the other treated groups (Table 2).

Effects of Imatinib, PRP mono-therapies and combination on the fibrotic score, hydroxyproline content, and liver histopathology:

Marked inflammation, necrosis, and macrovesicular/microvesicular steatosis were caused by CCl_4 administration for 9 weeks caused. According to the section which was stained by Masson's trichrome stains (Fig. 1), the fibrotic area score was significantly increased in group II compared to the control group. Fibrosis was significantly reduced in the groups which were treated with PRP, Imatinib, and combined therapy. The treatment with combined therapy showed a significant decrease in the score of the fibrotic area than the other treated groups (Fig. 2A).

A significant elevation in hydroxyproline content was caused by CCl_4 administration compared to the control group. PRP, Imatinib, and combined therapy significantly reduced the hydroxyproline content compared to the CCl_4 group. The treatment with combined therapy showed a significant decrease in the content of hydroxyproline than the other treated groups (Table 2).

Effects of Imatinib, PRP mono-therapies, and combination on the apoptotic marker (PI staining):

Propidium iodide (PI) marker showed that CCl_4 administration caused a significant elevation in necrotic cell percentages in comparison with the control. PRP, Imatinib and combined therapy treatments significantly decreased necrotic cell percentages compared with the CCl_4 group. Combined therapy treatment showed a more significant decrease in the necrotic cells' percentage than in the other treated groups (Fig. 2B).

Effects of Imatinib, PRP mono-therapies and combination on IL6, ASMA, and HGF gene expression:

The administration of CCl_4 caused a significant elevation in ASMA and IL6 levels and a significant reduction in HGF levels in comparison with the control group. PRP, Imatinib and combined therapy treatments significantly decreased ASMA and IL6 levels and significantly increased HGF levels in comparison with the CCl_4 group. The treatment with combined therapy showed a more significant decrease in ASMA and IL6 levels and a more significant increase in HGF levels than the other treated groups (Fig. 3).

Effects of Imatinib, PRP mono-therapies, and combination on hepatic oxidative stress parameters:

A significant elevation in MDA, NO, NOS, and MCP-1 was caused by the administration of CCl_4 compared to the control group. Treatment with PRP, Imatinib and combined therapy significantly decreased

the hepatic NO, NOS, MDA, and MCP-1 in comparison with the CCl_4 group. The combined therapy showed a more significant decrease in NO, MDA, NOS, and MCP-1 than the other treated groups (Table 2). Also, CCl_4 caused a marked reduction in the activity of SOD and catalase and a decrease in the content of GSH compared to the control group. PRP, Imatinib, and combined therapy treatment significantly elevated hepatic SOD, GSH, and catalase compared to CCl_4 group. The combined therapy showed a more significant elevation in SOD and catalase activity and a more significant increase in GSH content than the other treated groups (Table 2).

Discussion:

Our study revealed that Imatinib and PRP combination had a significantly superior antifibrotic eff ect than each treatment alone. There was a significant decrease in hydroxyproline, IL-6 and ASMA gene expression, MCP-1, ALT, MDA, NO, NOS, and significant increase of ALB, SOD, GSH, CAT, and HGF gene expression in the combined therapy group compared to each treatment alone. A possible mechanism by which Imatinib may synergize with PRP to execute more antifibrotic activity against the activated HSCs in rats (Fig. 4).

Our study revealed that CCl4 administration cause elevation in oxidative stress, hepatic hydroxyproline, caspase 3, MDA, NO, MCP-1, and NOS levels in addition to the decrease of GSH, SOD, and catalase levels. The change severity was associated with the hepatic injury degree and confirmed by the increase of liver function tests (ALT & albumin), and by the deviations in liver histopathology. This study also revealed that the administration of CCl4 caused elevation of IL-6 and ASMA gene expression and reduction of HGF gene expression and increase of PI staining.

The mechanism of hepatic oxidative stress which is caused by CCl_4 is started by trichloromethyl radical (•CCl3) [24]. •CCl3 forms a covalent bond to cell components, such as GSH, inhibits the secretion of lipoprotein, so steatosis occurs. Agreed with our results •OOCCl3 starts the lipid peroxidation with the formation of byproducts such as 4-HNE and MDA leading to loss of cell membrane integrity and cell death [25].

Some studies reported that NO and NOS have a role in hepatic fibrosis. NO stimulates guanylyl cyclase leading to formation of cGMP, that binds to cGMP-dependent protein kinases and stimulates a series of reactions that enable numerous biological mechanisms like platelet aggregation and vasodilation. iNOS-derived NO acts through these several pathways leading to the development and maintenance of several liver diseases [26] Parallel to our results the activities of SOD, CAT were showed to be lower in liver cirrhosis than normal liver tissue [27]. Those changes were associated with a decrease in GSH levels in cirrhotic liver tissue than healthy liver tissue.

A variety of parallel studies reported that the macrophages triggered by MCP-1 to the tissue injury site and the adhesion molecules, IL-1β, TNFα, and IL-6 are regulated by MCP-1 [28]. Moreover, MCP-1 had a role in the early liver injury or hepatic steatosis. There are other studies also established that MCP-1 stimulates lipid aggregation in cultures of hepatocytes. Overall, MCP-1 appears to have a significant role in liver steatosis and inflammatory responses during tissue damage [29].

Our results were parallel with others' reports who informed that the hepatocytes apoptosis causes the enrollment of inflammatory cells to the damaged liver tissues and the release of cytokines such as IL-6 and TGF-β1. TGF-β1 is vital to activate the myofibroblasts, which

leads to upregulation of α-smooth muscle actin (α-SMA) and the release of extracellular matrix proteins (e.g. collagen type I) [30]. HGF act as an effective mediator of cellular migration, proliferation, survival, and tissue regeneration. Additionally, HGF lowers the TGF-β1 expression and helps ECM degradation cause anti-fibrogenic properties [31].

PRP releases many mediators like cytokines and growth factors into the injured areas for initiating their recovery by increasing the proliferation viable cells [32]. PRP possesses an antifibrotic effect on the liver and ameliorates hepatotoxicity by reduction of intracellular oxidation and up-regulation of phosphorylated ERK1/2 and Akt pathways [33]. The platelets impact for regeneration in the liver includes three different mechanisms: a direct influence on hepatocytes, a favorable effect on liver sinusoidal endothelial cells, and a positive effect on Kupffer cells. Consequently, it is anticipated that the platelets expansion stimulated by platelet transfusion would improve liver functions in patients with chronic liver diseases [34]**.** Also, PRP suppresses HSCs activation and promotes HSCs apoptosis in the mice's liver [35]**.** Furthermore, PRP has a high level of ATP and ADP which are got degradation by HSCs giving adenosine so increasing cAMP inside HSCs leading to HSCs inactivation [36]**.**

PRP suppresses caspase-3 expression and secretes matrix metalloproteinase-9 (MMP-9) initiating HSCs apoptosis [37]**.** Previous studies showed that NO levels significantly decreased with PRP treatment [38]**.** PRP can reverse the oxidative stress by reducing the expression of iNOS leading to the inhibition of HSCs. In addition, NO can dilate the blood vessels leading to an increment of blood flow with low inflammatory cell infiltration [39]**.**

This PRP antifibrotic outcome agrees with Watanabe et al. who proved that thrombocytosis, actuated with thrombopoietin, reduced the percentage of fibrosis and hydroxyproline content in liver fibrosis [40]. PRP highly decreased the fibrotic area and the levels of hydroxyproline in hepatic fibrosis in severe combined immunodeficiency mice [41]. Since the levels of hydroxyproline is a specific marker for deposition of collagen and fibrosis [42], PRP decreases collagen deposition.

Our findings were in agreement with previous studies [43,44] who found that instant contact between hepatocytes and platelets could induce several cytokines and growth factors release like TGF-α, HGF, IL-6, TNF-α, and IGF-1, which have essential roles in liver recovery. The growth factors induce hepatocyte mitosis, which finally causes liver recovery. PRP protects the liver against histological deformations and attenuated oxidation [44]. Furthermore, our results were inconsistence with [41] who reported that PRP could reduce a-SMA. Also, our findings were parallel with another report, that proved the liver functions improvement in mice that injected with PRP could be due to a reduction in liver fibrosis, amelioration of the oxidative status of the hepatocytes, and regeneration of injured hepatocytes [45].

On the other hand, Imatinib significantly prevents HSCs activation and proliferation as well as stimulates apoptosis of HSCs in vivo and in vitro, where mitochondrial activity and superoxide anion synthesis showed marked depletion with imatinib administration. Also, cDNA microarray showed a significant up-regulation of interleukin-6 and mRNA genes, in addition to stimulation of IL-6 secretion.Our results agreed with previous findings by [46] who reported that Imatinib inhibited collagen type (I) gene expression, β-PDGFR, ASMA, MMP2, and TGFβ-1.

Our study strength was the usage of two different treatments which had a safe synergetic effect and can be used in clinical trials in further studies. Also, the image analysis of fibrotic areas in this study was a suitable proof for appropriate assessment of the antifibrotic effect of these treatments and enabled more precise evaluation. The limitation of this study was that it is an experience in a single centre that requires authentication in other centres.

Conclusion:

Eventually, we deduce that PRP synergized with Imatinib to perform a safer and more effective anti-fibrotic effect against liver fibrosis with a minimum cytotoxic effect on normal cells. Hence, new strategies of therapeutics for the treatment of liver fibrosis including the combined therapy of PRP and Imatinib could be developed. As well, studies on long-term toxicity are required for discovering any long-term side effects regarding this combined treatment.

Ethics declarations

Competing interests

The authors state that they haven't competing interests.

Funding

No funding was received for conducting this study

Ethical approval and participation consent

The protocol of this research fulfilled the International Ethical Guidelines for Biomedical Research [47]. All rats had a good care according to the National Institutes of Health criteria for care of laboratory animals. Beni-Suef University, Egypt, approved all procedures (BSU/2021/4).Written consent was given by all authors in the study.

Data availability

The data which supports this study are available upon request.

Authors' contributions

All authors contributed equally to all parts of this study.

References:

1. Aydın MM, Akçalı KC. Liver fibrosis. Turk J Gastroenterol. 2018;29(1):14-21.

2. Wang P, Pu Y, Li H, et al. Prognosis for recipients with hepatocellular carcinoma of salvage liver transplantation versus those of primary liver transplantation: a retrospective single-center study. SpringerPlus. 2016 2016/10/18;5(1):1809.

3. Etulain J. Platelets in wound healing and regenerative medicine. Platelets. 2018 2018/08/18;29(6):556-568.

4. Chellini F, Tani A, Vallone L, et al. Platelet-Rich Plasma Prevents In Vitro Transforming Growth Factor-β1-Induced Fibroblast to Myofibroblast Transition: Involvement of Vascular Endothelial Growth Factor (VEGF)-A/VEGF Receptor-1-Mediated Signaling (†). Cells. 2018;7(9):142.

5. Shoeib HM, Keshk WA, Foda AM, et al. A study on the regenerative effect of platelet-rich plasma on experimentally induced hepatic damage in albino rats. Canadian Journal of Physiology and Pharmacology. 2018 2018/06/01;96(6):630-636.

6. Elghblawi E. Platelet-rich plasma, the ultimate secret for youthful skin elixir and hair growth triggering. Journal of Cosmetic Dermatology. 2018 2018/06/01;17(3):423-430.

7. Heldin C-H. Targeting the PDGF Signaling Pathway in the Treatment of Non-Malignant Diseases.

Journal of Neuroimmune Pharmacology. 2014 2014/03/01;9(2):69-79.

8. Friedman SL. Mechanisms of hepatic fibrogenesis. Gastroenterology. 2008;134(6):1655-1669.

9. Nabil A, Elshemy MM, Asem M et al. Zinc Oxide Nanoparticle Synergizes Sorafenib Anticancer Efficacy with Minimizing Its Cytotoxicity. Oxid Med Cell Longev., 2020; 2020:1362104.

10. Nabil A, Uto K, Zahran F, et al. The Potential Safe Antifibrotic Effect of Stem Cell Conditioned Medium and Nilotinib Combined Therapy by Selective Elimination of Rat Activated HSCs. Biomed Res Int., 2021; 2021:6678913

11. Yoshiji H, Noguchi R, Kuriyama S, et al. Imatinib mesylate (STI-571) attenuates liver fibrosis development in rats. American journal of physiology Gastrointestinal and liver physiology. 2005 2005/05/01;288(5):G907-G913.

12. Tomizawa M, Shinozaki F, Sugiyama T, et al. Sorafenib suppresses the cell cycle and induces the apoptosis of hepatocellular carcinoma cell lines in serum-free media. Experimental and therapeutic medicine. 2010 2010/09//;1(5):863-866.

13. Shiha G, Nabil A, Lotfy A, et al. Antifibrotic Effect of Combination of Nilotinib and Stem Cell-Conditioned Media on CCl4-Induced Liver Fibrosis. Stem Cells Int., 2020; 2020:6574010.

14. Nabil A, Elshemy MM, Asem M, et al. Protective Effect of DPPD on Mercury Chloride-Induced Hepatorenal Toxicity in Rats. 2020;2020.

15. Gérard-Monnier D, Erdelmeier I, Régnard K, et al. Reactions of 1-Methyl-2-phenylindole with Malondialdehyde and 4-Hydroxyalkenals. Analytical Applications to a Colorimetric Assay of Lipid Peroxidation. Chemical Research in Toxicology. 1998 1998/10/01;11(10):1176-1183.

16. Miranda KM, Espey MG, Wink DA. A Rapid, Simple Spectrophotometric Method for Simultaneous Detection of Nitrate and Nitrite. Nitric Oxide. 2001 2001/02/01/;5(1):62-71.

17. Marklund S, Marklund G. Involvement of the Superoxide Anion Radical in the Autoxidation of Pyrogallol and a Convenient Assay for Superoxide Dismutase. European Journal of Biochemistry. 1974 1974/09/01;47(3):469-474.

18. Johansson LH, Håkan Borg LA. A spectrophotometric method for determination of catalase activity in small tissue samples. Analytical Biochemistry. 1988 1988/10/01/;174(1):331-336.

19. Farrokhfall K, Hashtroudi MS, Ghasemi A, et al. Comparison of inducible nitric oxide synthase activity in pancreatic islets of young and aged rats. Iran J Basic Med Sci. 2015;18(2):115-121.

20. Smith IK, Vierheller TL, Thorne CA. Assay of glutathione reductase in crude tissue homogenates using 5,5′-dithiobis(2-nitrobenzoic acid). Analytical Biochemistry. 1988 1988/12/01/;175(2):408-413.

21. Kumar Ajith G, Ballantyne Christie M, Michael Lloyd H, et al. Induction of Monocyte Chemoattractant Protein-1 in the Small Veins of the Ischemic and Reperfused Canine Myocardium. Circulation. 1997 1997/02/04;95(3):693-700.

22. Riccardi C, Nicoletti I. Analysis of apoptosis by propidium iodide staining and flow cytometry. Nature Protocols. 2006 2006/08/01;1(3):1458-1461.

23. Liu S-J, Wang P, Jiao J, et al. Differential gene expression associated with inflammation in peripheral blood cells of patients with pneumoconiosis. J Occup Health. 2016;58(4):373-380.

24. Ruch RJ, Klaunig JE, Schultz NE, et al. Mechanisms of chloroform and carbon tetrachloride toxicity in primary cultured mouse hepatocytes. Environ Health Perspect. 1986;69:301-305.

25. Weber LWD, Boll M, Stampfl A. Hepatotoxicity and Mechanism of Action of Haloalkanes: Carbon Tetrachloride as a Toxicological Model. Critical Reviews in Toxicology. 2003 2003/01/01;33(2):105-136.

26. Iwakiri Y, Kim MY. Nitric oxide in liver diseases. Trends Pharmacol Sci. 2015;36(8):524-536.

27. Czeczot H, Scibior D, Skrzycki M, et al. Glutathione and GSH-dependent enzymes in patients with liver cirrhosis and hepatocellular carcinoma. Wiad Lek. 2006;53(1):237-241.

28. Lu B, Rutledge BJ, Gu L, et al. Abnormalities in monocyte recruitment and cytokine expression in monocyte chemoattractant protein 1-deficient mice. J Exp Med. 1998;187(4):601-608.

29. Mandrekar P, Ambade A, Lim A, et al. An essential role for monocyte chemoattractant protein-1 in alcoholic liver injury: regulation of proinflammatory cytokines and hepatic steatosis in mice. Hepatology (Baltimore, Md). 2011;54(6):2185-2197.

30. Meng F, Wang K, Aoyama T, et al. Interleukin-17 signaling in inflammatory, Kupffer cells, and hepatic stellate cells exacerbates liver fibrosis in mice. Gastroenterology. 2012;143(3):765-776.e3.

31. Vyas B, Ishikawa K, Duflo S, et al. Inhibitory effects of hepatocyte growth factor and interleukin-6 on transforming growth factor-beta1 mediated vocal fold fibroblast-myofibroblast differentiation. Ann Otol Rhinol Laryngol. 2010;119(5):350-357.

32. Masuki H, Okudera T, Watanebe T, et al. Growth factor and pro-inflammatory cytokine contents in platelet-rich plasma (PRP), plasma rich in growth factors (PRGF), advanced platelet-rich fibrin (A-PRF), and concentrated growth factors (CGF). International journal of implant dentistry. 2016 Dec;2(1):19.

33. Abdel Fattah SM, Saif-Elnasr M, Soliman AF. Platelet-rich plasma as a potential therapeutic approach against lead nitrate- and/or gamma

radiation-induced hepatotoxicity. Environmental Science and Pollution Research. 2018 2018/12/01;25(34):34460-34471.

34. Salem NA, Hamza A, Alnahdi H, et al. Biochemical and Molecular Mechanisms of Platelet-Rich Plasma in Ameliorating Liver Fibrosis Induced by Dimethylnitrosurea. Cellular physiology and biochemistry : international journal of experimental cellular physiology, biochemistry, and pharmacology. 2018;47(6):2331-2339.

35. Malik R, Selden C, Hodgson H. The role of non-parenchymal cells in liver growth. Seminars in cell & developmental biology. 2002 Dec;13(6):425-31.

36. Ikeda N, Murata S, Maruyama T, et al. Platelet-derived adenosine 5'-triphosphate suppresses activation of human hepatic stellate cell: In vitro study. Hepatology research : the official journal of the Japan Society of Hepatology. 2012 Jan;42(1):91-102.

37. Hemmann S, Graf J, Roderfeld M, et al. Expression of MMPs and TIMPs in liver fibrosis - a systematic review with special emphasis on anti-fibrotic strategies. J Hepatol. 2007 May;46(5):955-75.

38. Novokmet S, Jakovljevic VL, Jankovic S, et al. Human platelets perfusion through isolated guinea-pig heart: the effects on coronary flow and oxidative stress markers. 2009;28:98-104.

39. Hirata M, Hirata K, Kage M, et al. Effect of nitric oxide synthase inhibition on Schistosoma japonicum egg- induced granuloma formation in the mouse liver. 2001;23(6):281-289.

40. Watanabe M, Murata S, Hashimoto I, et al. Platelets contribute to the reduction of liver fibrosis in mice. 2009;24(1):78-89.

41. Takahashi K, Murata S, Fukunaga K, et al. Human platelets inhibit liver fibrosis in severe combined immunodeficiency mice. 2013;19(32):5250.

42. Elshemy MM, AbdEl-Mejied AE, Zahran F, et al. DPPD ameliorates renal fibrosis induced by HgCl2 in rats. 2018;15(3):2416-2425.

43. Ohkohchi N, Murata S, Takahashi KJIJH, doi. Platelet and Liver Regeneration, Tissue Regeneration—from Basic Biology to Clinical Application. 2012;10(2012):542479.

44. Hesami Z, Jamshidzadeh A, Ayatollahi M, et al. Effect of Platelet-Rich Plasma on CCl4-Induced Chronic Liver Injury in Male Rats. Int J Hepatol. 2014;2014:932930-932930.

45. Mafi A, Dehghani F, Moghadam A, et al. Effects of platelet-rich plasma on liver regeneration in CCl4-induced hepatotoxicity model. 2016;27(8):771-776.

46. Kim Y, Fiel MI, Albanis E, et al. Anti-fibrotic activity and enhanced interleukin-6 production by hepatic stellate cells in response to imatinib mesylate. Liver Int. 2012;32(6):1008-1017.

47. CIOMS/WHO. International Ethical Guidelines for Biomedical Research Involving Human Subjects. Geneva: CIOMS. 1993.

Figure legends

Fig. 1. Histopathological examination of liver tissues among the studied groups (magnification ×400). (A) Control group: collagen fibers can't be seen. (B) Collagen accumulation in the liver tissues of CCl_4 group. A significant reduction in collagen was detected in rats treated with Imatinib (C), PRP (D) as monotherapy, and in combination (E) with the highest decrease in collagen content detected in the combination group.

Fig. 2. Effects of Imatinib, PRP mono-therapies, and in combination on fibrosis score (Fig. 2A) and necrotic% (Fig. 2B). All samples were measured independently in triplicate. Significant differences are indicated as: a: significant compared to the control group; b: significant compared to CCl_4 group; c: significant compared to CCl_4+ Imatinib group; d: significant compared to CCl_4+PRP group.

Fig. 3. Effects of Imatinib, PRP mono-therapies, and in combination on ASMA (Fig. 3A), IL6 (Fig. 3B) and HGF (Fig. 3C) gene expression levels. Significant differences are indicated as: a: significant compared to the control group; b: significant compared to CCl_4 group; c: significant compared to CCl_4+ Imatinib group; d: significant compared to CCl_4+PRP group.

Fig. 4. The proposed mechanism by which PRP synergized Imatinib liver anti-fibrotic effect.

Table (1): PCR primer sequences for IL6, HGF, and ASMA

Gene Symbol	Primer sequence
IL6	5'-CAAATTCGGTACATCCTC-3' (F) 5'-CTGGCTTGTTCCTCACTA-3' (R)
HGF	TCT CGT TGT GAA GGT GAT AC (F) TGG TCC TGA TCC AAT CTT CT (R)
ASMA	5′-GAGCGTGGCTATTCCTTCGTG-3′ (F) 5′-CAGTGGCCATCTCATTTTCAAAGT-3′ (R)

Table 2: Biochemical and oxidative stress parameters:

Parameters	Control	CCl_4	CCl_4+ Imatinib	CCl_4+ PRP	CCl_4+ combination	P
Serum:						
ALT (U/L)	26.6±3.1	70.2±11.9[a]	45.2±8.2[a,b]	40.2±8.9[b]	28.8±5.1[b, c]	<0.001**
ALB (g/dL)	4.1±0.1	2.3±0.6[a]	3.3±0.7[b]	3.4±0.2[b]	4±0.2[b]	<0.001**
Homogenate:						

Hydroxyproline (ug/mg tissue)	20.7±2.1	89.6±11.5[a]	43.6±5.1[a,b]	61.3±9.2[a,b,c]	24.8±3.4[b,c,d]	<0.001**
MDA (mmol/g tissue)	51.1±6.3	137.3±6.9[a]	76.3±8.1[a,b]	81.9±10.9[a,b]	58.2±7.9[b,c,d]	<0.001**
GSH (µmol/g protein)	25.5±1.7	10.9±2.7[a]	20.4±2.5[b]	21.9±2.7[b]	23.6±3.5[b]	<0.001**
NO (µmol/g)	157.1±12.5	290.4±21[a]	184.5±18.7[b]	178.2±13.5[b]	161.9±11.6[b]	<0.001**
NOS (Pmol/min/mg protein)	17.3±2.7	29.1±4.1[a]	18.8±4.7[b]	19.7±3.2[b]	18.1±2.9[b]	<0.001**
SOD (U/mg protein)	22.4±2.3	11.2±2.9[a]	18.7±2.1[b]	19.4±2.5[b]	21.4±1.9[b]	<0.001**
CAT (mol/min/gm)	1.11±0.18	0.54±0.14[a]	0.98±0.25[b]	0.92±0.21[b]	1.07±0.24[b]	<0.001**
MCP-1 (Pg⁄ml)	462.6±67.3	760.1±107[a]	580.8±76.2[a,b]	543±64[a,b]	471±75[b,c,d]	<0.001**

P: Probability **: High significance

[a] Significant compared to the control group. [b] Significant compared to CCL4 group.

[c] Significant compared to CCl4+ Imatinib group. [d] Significant compared to CCl4+PRP group.

Fig.1

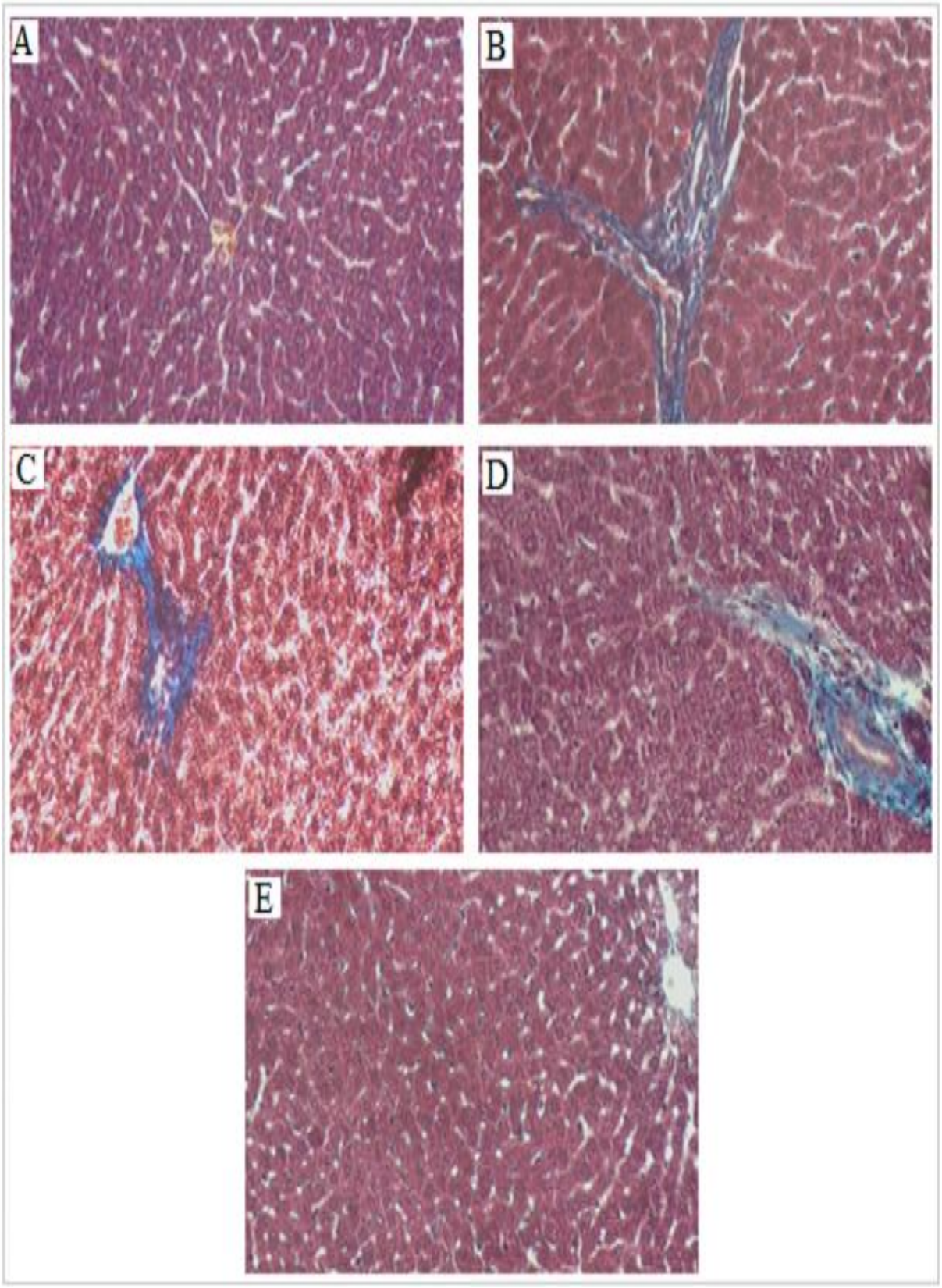
A
B
C
D
E

Fig. 2

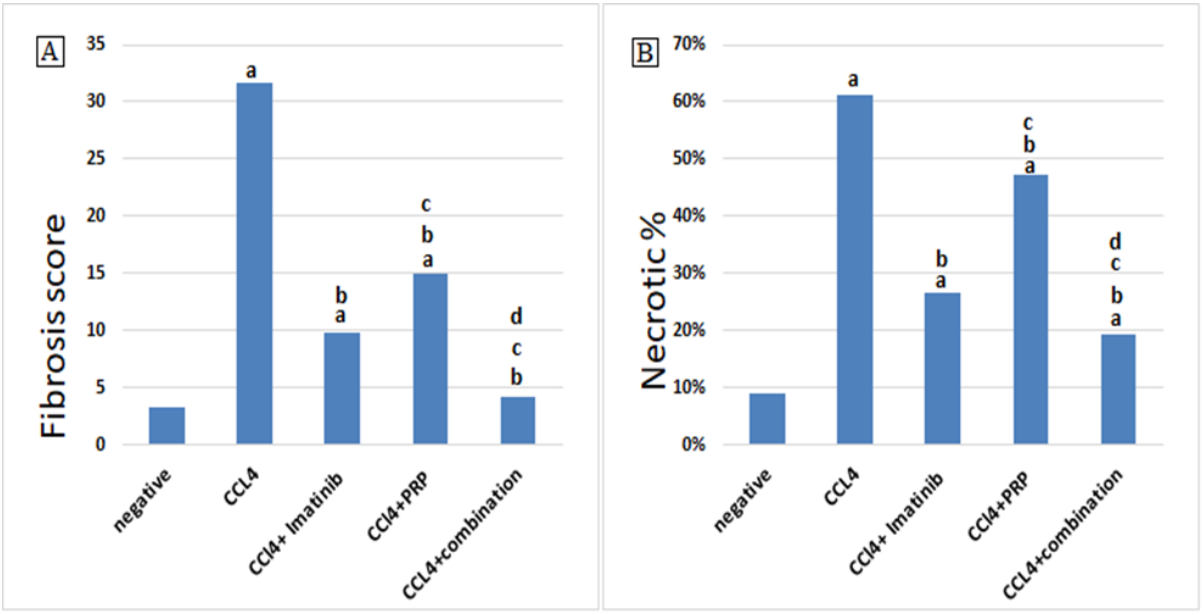

Fig. 3

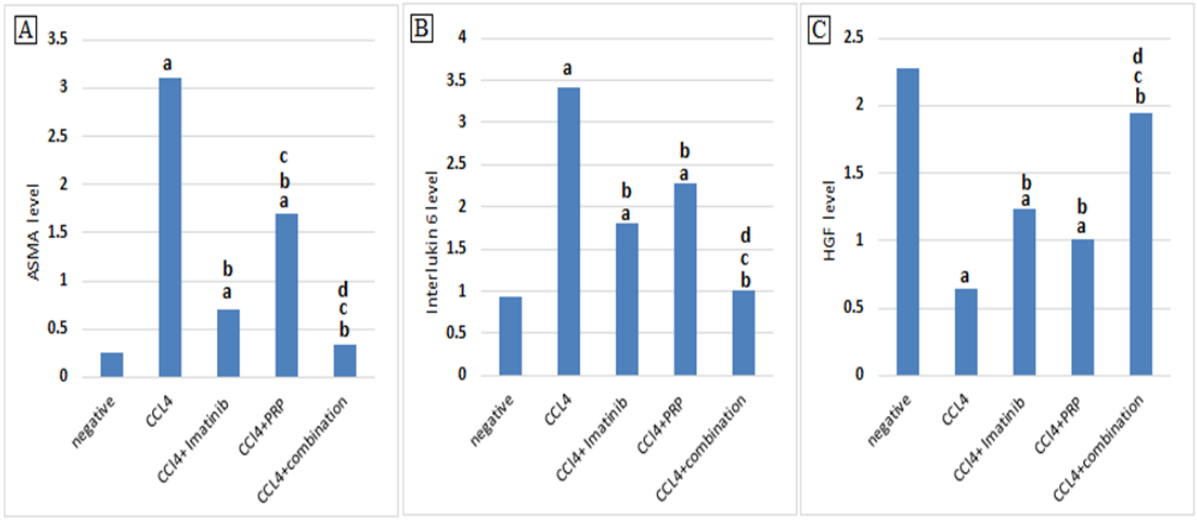

Fig. 4

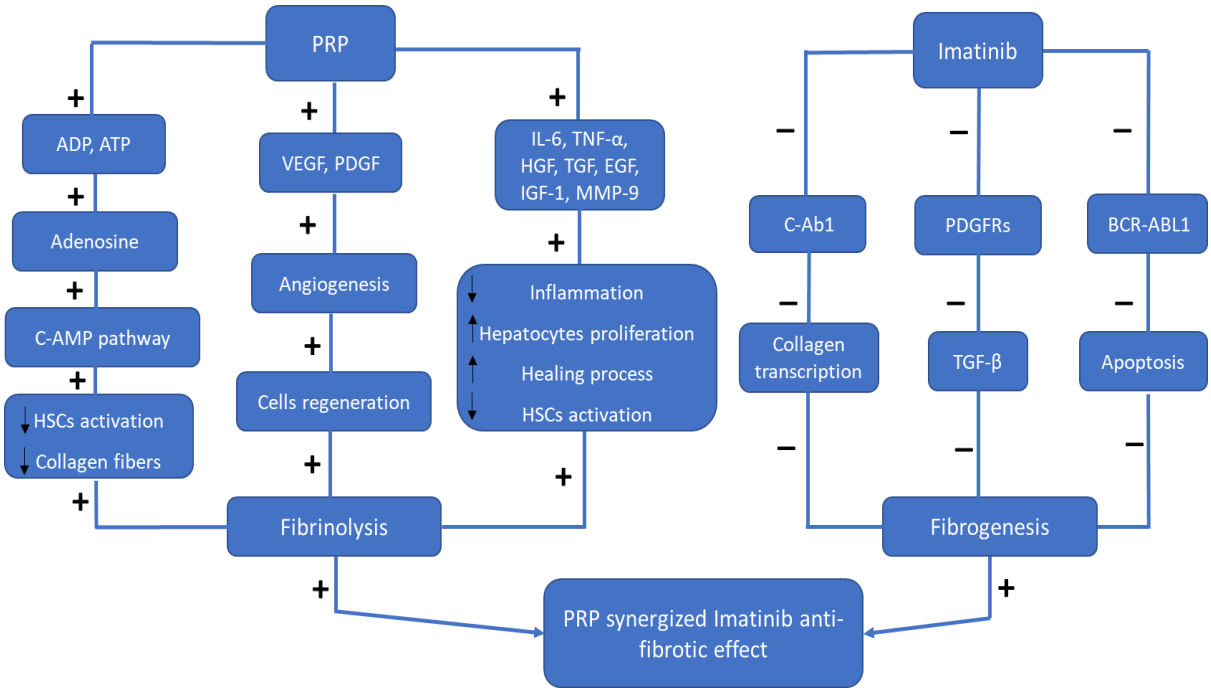
PRP
ADP, ATP
Adenosine
C-AMP pathway
HSCs activation
Collagen fibers
VEGF, PDGF
Angiogenesis
Cells regeneration
IL-6, TNF-α, HGF, TGF, EGF, IGF-1, MMP-9
Inflammation
Hepatocytes proliferation
Healing process
HSCs activation
Fibrinolysis
Imatinib
C-Ab1
Collagen transcription
PDGFRs
TGF-β
BCR-ABL1
Apoptosis
Fibrogenesis
PRP synergized Imatinib anti-fibrotic effect